Available online at www.sciencedirect.com
ScienceDirect
J. Mater. Sci. Technol., 2010, **26**(10), 945-950.
JMST
www.JMST.org

Mechanically Assisted Electroless Barrel-plating Ni-P Coatings Deposited on Carbon Steel

Zhaoxia Ping[1)†], *Guoan Cheng*[1)] *and Yedong He*[2)]

1) Key Laboratory of Beam Technology and Material Modification of Ministry of Education, College of Nuclear Science and Technology, Beijing Normal University, Beijing 100875, China
2) Beijing Key Laboratory for Corrosion, Erosion and Surface Technology, University of Science and Technology Beijing, Beijing 100083, China

[Manuscript received October 30, 2009, in revised form February 23, 2010]

A mechanically assisted electroless (MAE) barrel-plating technique has been developed to deposit Ni-P coatings on carbon steel. The mechanical treatment was carried out in a rolling drum containing carbon steel specimens and glass balls of 2–3 mm diameter, which was submerged in a bath containing electroless plating solution. The coatings are Ni-polycrystalline and have a fine grained structure and smooth surfaces. The hardness and corrosion resistance of the novel coatings are considerably improved compared with the conventional electroless (CE)-plated Ni-P coatings, which are amorphous. After heat treatment at 400°C for one hour, cracks and pores are observed in the CE-plated Ni-P coating, while no cracks appear in the MAE barrel-plated Ni-P coating. The improved properties of the MAE barrel-plated Ni-P coatings demonstrate the advantages of this novel technique, wide applications of which will be found in industries.

KEY WORDS: Mechanically assisted electroless barrel-plating; Ni-P coating; Crystallization; Corrosion resistance; Microhardness

1. Introduction

Electroless-plated nickel-phosphorus (Ni-P) coatings have been widely used in various industries[1–3]. The electroless-plating process and post-plating heat treatment determine the Ni-P coating composition and microstructure, which have attracted intensive interest from academia and industries[4–10]. Amorphous Ni-P coatings are formed in electroless-plating when the P content is higher than 8 wt pct[11]. If the amorphous coatings are crystallized, the mechanical properties of Ni-P coatings will be greatly improved[4–9,12,13]. Crystallization of amorphous Ni-P coatings is usually achieved by post-plating heat treatment. Cracking of Ni-P coatings generally occurs during the heat treatment because the specific density of the Ni-P coating in the amorphous phase is smaller than that in the crystalline phase[14]. Cracks degrade the corrosion resistance of the Ni-P coating and other crack-related mechanical properties[15]. Crystalline Ni-P coatings free of cracks are desired for industrial applications. How to produce the desired Ni-P coatings is a challenging issue. The present study explores a mechanically assisted electroless (MAE) barrel-plating technique to achieve this goal.

There are three ways to apply mechanical attrition action, which are vibrating the glass balls in horizontal or vertical directions and stirring the solution containing specimens and ceramic balls. But these methods have many limitations: horizontal and vertical vibrations are only applicable for single-sided electroplating and electroless-plating; the method of stirring is only suitable for the electroless-plating of small samples. So a new method of mechanical attrition treatment should be adopted.

Barrel-plating methods are applicable for electroplating. It was originated in the post-Civil War era and the equipment was readily adapted from available wooden barrels, kegs, or baskets[16]. Great advances in plating-barrel performance, capability, and longevity were the result of plastic materials newly available after World War II. Prior to that time, plating barrels were known to be composed of more primitive plastic or phenolic materials. Today, the sub-

† Corresponding author. Tel.: +86 10 62205403; Fax: +86 10 62205403; E-mail address: pingzx@yeah.net (Z.X. Ping).

Table 1 Composition of the plating solution and plating parameters

Plating solution composition/(g/L)				Electroless parameters		
$NiSO_4{\cdot}6H_2O$	$NaH_2PO_2{\cdot}H_2O$	$NaCH_3COO{\cdot}H_2O$	$C_6H_5Na_3O_7{\cdot}2H_2O$	pH	Temperature	Time
25	20	5	5	5.5	80°C	1 h

merged portions of barrel-plating equipment are composed, as much as possible, of nonconductive, chemically inert materials that can be utilized in various acid and alkaline solutions.

The mechanical attrition produced by stirring the solution containing balls has been reported in literature [17]. Compared with stirring method, mechanically assisted barrel-plating have some advantages. Firstly, the mechanically assisted barrel-plating coatings could be deposited on the big samples. Secondly, the coating of mechanically assisted barrel-plating is uniform, and the quality of the coating is improved greatly. Thirdly, the fluctuation of the coating thickness is little, while the thickness of the coating is nonuniform after stirring. Therefore, mechanically assisted barrel-plating must have active significance on the area of electroless plating.

In the present research, we applied mechanical attrition to the barrel-plating Ni-P coatings on magnesium alloy to modify the microstructure and properties of the coatings.

2. Experimental

The MAE barrel-plating set-up is schematically shown in Fig. 1. Samples to be plated were carbon steel with dimension of 20 mm×10 mm×2 mm. The sample surfaces were ground with SiC papers to 1200 grit. The composition of the plating solution and plating parameters are listed in Table 1. Before depositing, the sample was first degreased ultrasonically in ethanol for 5 min, rinsed with deionized water, and then immersed in 5% dilute hydrochloric acid for 30–60 s and rinsed again with deionized water thoroughly. MAE-plating and CE-plating were all carried out at 80°C and each plating process lasted for 1 h. Some plated samples were annealed at 400°C for 1 h to investigate the cracking phenomenon induced by crystallization.

X-ray diffraction analysis (XRD, PW3710, Philips, The Netherlands) was conducted to characterize crystal structures of the as-deposited coatings and the coatings after heat treatment. The surface and cross-sectional morphologies of coatings were examined by scanning electron microscopy (SEM, JSM-6480LV, JEOL, Japan). Chemical compositions of the coatings were analyzed with an X-ray energy dispersive spectroscope attached in the SEM. Hardness of the coatings was measured by using a digital microhardness tester (HVS-1000) with a load of 2.94 N and a duration time of 20 s. At least ten indents were performed to gain average hardness value for each sample.

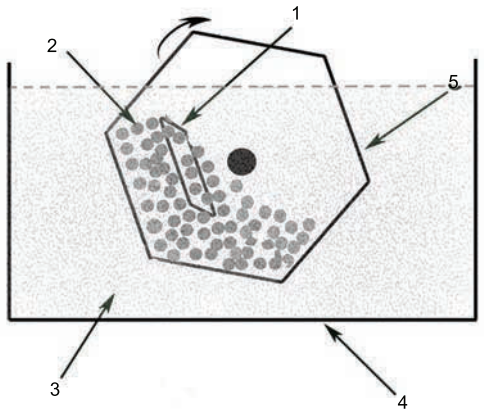

Fig. 1 Schematic diagram of mechanically assisted electroless barrel-plating set-up: 1—sample, 2—ball, 3—bath solution, 4—coating bath, 5—rolling drum

The anodic polarization and electrochemical impedance spectroscopy (EIS) tests were performed on a galvano-chemistry Workstation (CHI660C, Shanghai, China) in 3.5% NaCl solution at room temperature by using a three-electrode electrochemical cell with a platinum plate as the counter-electrode and a saturated calomel electrode (SCE, +242 mV *vs* NHE) as the reference electrode. Each of the samples exposed a testing area of 1 cm^2 to the solution and the rest part was covered by an anticorrosion tape. The EIS spectra were obtained over the frequency range of 10 mHz–100 kHz with an applied AC perturbation potential of 10 mV amplitude. The EIS data were simulated with Boukamp′s algorithm implemented in Zsimpwin software. The average surface roughness (R_a) of the as-deposited coatings was determined by using an optical profiler (Wyko NT3300, Vecco, Germany) in vertical scanning interferometry (VSI) mode. The scanning area and vertical resolution in the VSI mode were 155 μm×204 μm and 1 nm, respectively. The surface roughness of the plated coatings was measured in at least five places and the average value was reported here.

3. Results and Discussion

3.1 Surface morphology

Figure 2(a)–(d) show the surface SEM morphologies of the Ni-P coatings on carbon steel electroless-plated without and with mechanical assistance, respectively. The MAE barrel-plated Ni-P coating has a much smoother surface than the conventional electroless (CE)-plated Ni-P coating. Although both Ni-

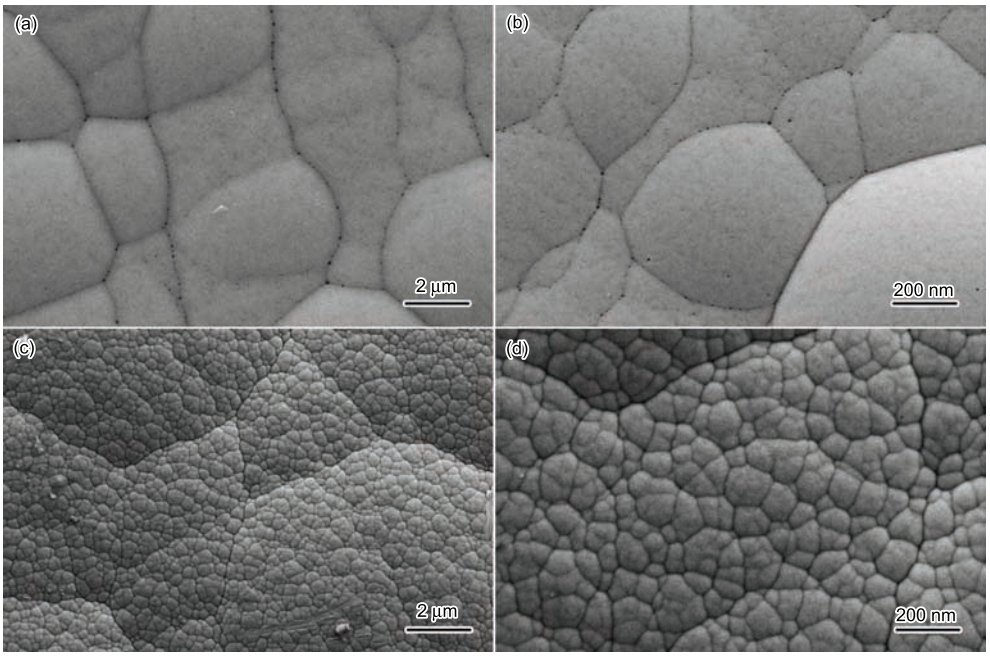

Fig. 2 Surface morphologies of Ni-P coatings on carbon steels electroless plated without ((a) and (b)) and with ((c) and (d)) mechanical assistance

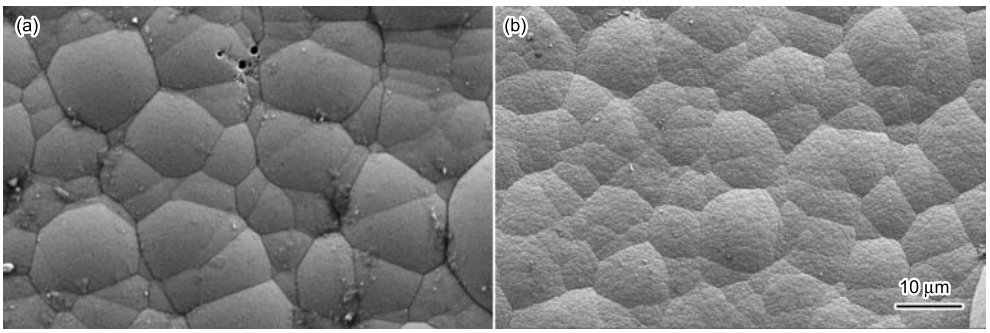

Fig. 3 Surface morphologies of CE-plated (a) and MAE barrel-plated (b) Ni-P coatings on carbon steels after heat treatment at 400°C for 1 h

P coatings exhibit the typical "cauliflower-like" surface, the size of the "cauliflower-like" cluster is below 100 nm on the MAE barrel-plated Ni-P coating surface, while it is about 5–20 μm on the electroless-plated Ni-P coating surface. The average surface roughness (R_a) of the MAE barrel-plated coating is about 85.00 nm, which is much smaller than that of the CE-plated coating (310.76 nm). The MAE barrel-plating process makes the coating surface smoother.

After heat treatment at 400°C for 1 h, the surface morphology is much different between the CE-plated coatings and the MAE barrel-plated coatings, as shown in Fig. 3(a) and (b). Cracks and pores appear on the surface of the CE-plated coatings, while no cracks are found on the surface of the MAE barrel-plated Ni-P coatings. In addition to cracks, small pores are formed in the CE-plated Ni-P coating, as shown in Fig. 3(a). No pores are observed on the surface of the MAE barrel-plated Ni-P coating (Fig. 3(b)). By comparing Fig. 3(b) with Fig. 2(d), it can be seen that the surface morphology of the MAE barrel-plated Ni-P coating remains almost unchanged after heat treatment. The MAE barrelplating technique solves the severe cracking and pores problem of Ni-P coatings.

Figure 4(a) and (b) are SEM images of the cross-section of the Ni-P coatings produced by electroless-plated without and with mechanical assistance, respectively. Under the same plating condition, the thickness of the CE-plated coating is about 20 μm, whereas the thickness of the MAE barrel-plated Ni-P coating is about 15 μm. Mechanical *in situ* treatment makes the Ni-P coating become thinner by about 5 μm. In addition, the interface roughness between the carbon steel substrate and the Ni-P coating is reduced by the mechanical *in situ* treatment.

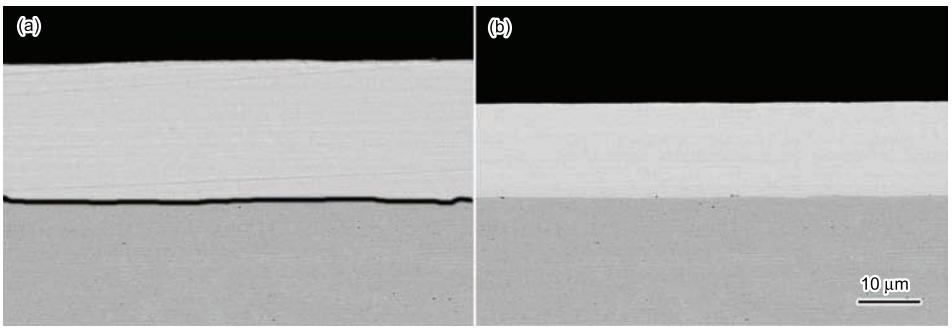

Fig. 4 Cross-section SEM images of Ni-P coatings on carbon steel by CE-plating (a) and MAE barrel-plating (b)

3.2 Composition and phase analysis

EDS analysis indicates that the P content is about 13.5 wt pct in the CE-plated Ni-P coating and about 10.1 wt pct in the MAE barrel-plated Ni-P coating. When the P content is higher than 8 wt pct[11], Ni-P coatings are usually amorphous. As expected, the CE-plated Ni-P coating without heat treatment is amorphous, as proved by the XRD pattern (Fig. 5(a)). The MAE barrel-plating produces crystalline Ni-P coating, as indicated by the XRD pattern (Fig. 5(b)), where only the face-centered cubic (fcc) Ni peaks are visible. After heat treatment, the conventional electroless plated Ni-P coating and the electroless-plated with mechanical assistance Ni-P coating are fully crystallized into Ni and Ni_3P phases as shown in Fig. 5(a) and (b).

3.3 Microhardness

The microhardness test results show that the CE-plated and MAE barrel-plated Ni-P coatings have the mean microhardnesses of 350±10 and 485±10 HV, respectively. The mechanical *in situ* treatment increases the microhardness of the Ni-P coating by about 135 HV, thereby indicating that the wear resistance of the Ni-P coating will be greatly improved. After heat treatment, the microhardness of CE-plated Ni-P coating is 580±10 HV, while the microhardness of MAE barrel-plated Ni-P coating is increased to 770±10 HV. The average grain size, d, of Ni and Ni_3P might be estimated from the full width of half maximum (FWHM) of the XRD peak *via* the Scherrer equation[18]:

$$d_{\mathrm{XRD}} = \frac{k\lambda}{\beta(\theta)\cos\theta} \tag{1}$$

where λ is the X-ray wavelength, β is the FWHM of the diffraction peak, θ is the diffraction angle and the constant $k\approx1$. From the XRD patterns indicated in Fig. 5 and using Eq. (1), we estimate the average grain sizes of Ni and Ni_3P in the MAE barrel-plated Ni-P coating to be 28 and 32 nm, respectively, which are correspondingly smaller than the average grain sizes of Ni and Ni_3P in the CE-plated Ni-P coating, 320 nm for Ni and 210 nm for Ni_3P. That might be the reason why the MAE barrel-plated Ni-P coating

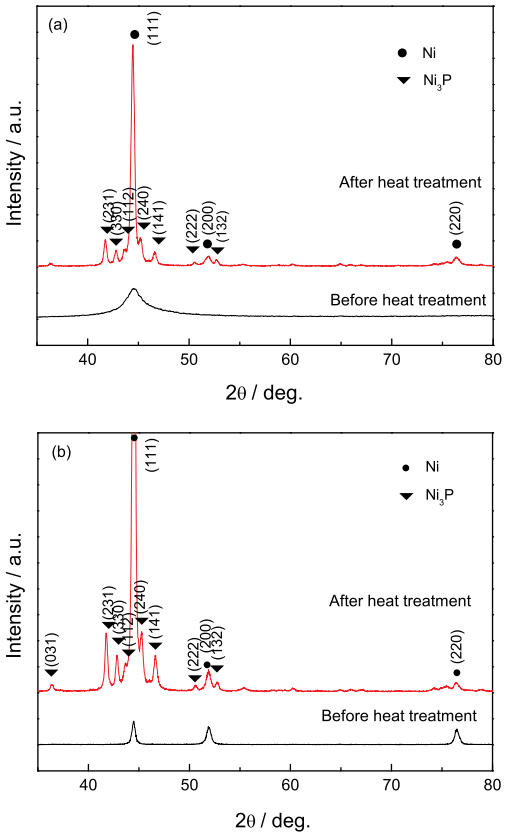

Fig. 5 Comparison of XRD patterns for CE-plated Ni-P coating (a) and MAE barrel-plated Ni-P coating (b) before and after heat treatment

after heat treatment exhibits enhanced microhardness compared with the CE-plated Ni-P coating after the same annealing process.

3.4 Electrochemical testing

Figure 6 shows the polarization curves of the CE-plated Ni-P coatings and MAE barrel-plated Ni-P coatings before and after heat treatment, and the carbon steel substrate in 3.5% NaCl solution at room temperature. The carbon steel has the most negative corrosion potential E_{corr} among the studied samples. Before heat treatment, the E_{corr} of the MAE barrel-plated Ni-P coating is higher than that of the CE-

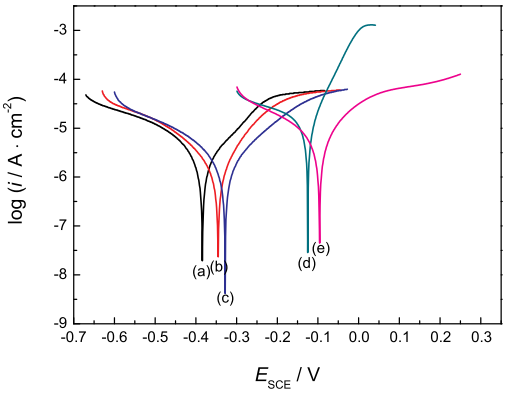

Fig. 6 Polarization curves in 3.5% NaCl solution at room temperature: (a) carbon steel substrate, (b) CE-plated coating after heat treatment, (c) CE-plated coating before heat treatment, (d) MAE barrel-plated coating after heat treatment, (e) MAE barrel-plated coating before heat treatment

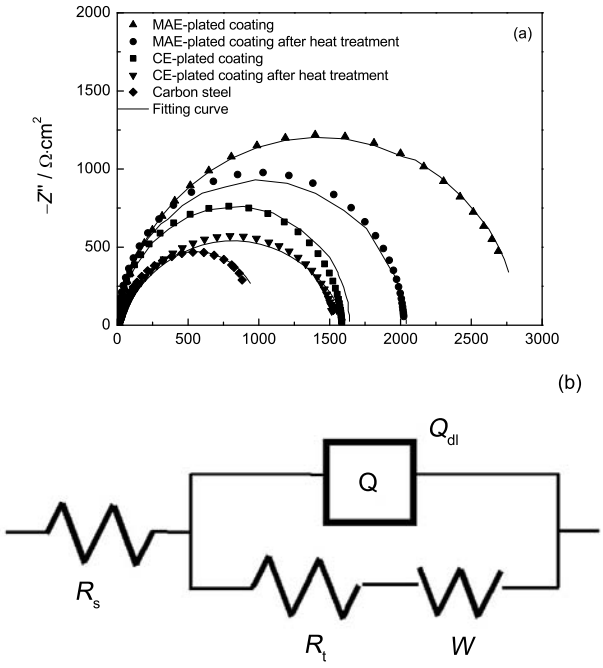

Fig. 7 (a) Nyquist plots for carbon steel substrate, CE-plated and MAE barrel-plated Ni-P coatings before heat treatment and after in 3.5% NaCl solution at room temperature, respectively; (b) equivalent circuit for fitting the EIS data

plated Ni-P coating. After heat treatment, the E_{corr} of the MAE barrel-plated Ni-P coating is also higher than that of the CE-plated Ni-P coating. This result indicates that the corrosion resistance of the Ni-P coating is improved by the mechanical *in situ* treatment. After heat treatment, the corrosion potentials of the CE-plated coating and the MAE barrel-plated coating both shift negatively compared with their as-deposited status correspondingly, which might be caused by the change in microstructure such as crystallization and grain growth, as described above.

The measured EIS data in the Nyquist format are presented in Fig. 7(a). Figure 7(b) shows an equivalent circuit, which consists of a solution resistance (R_S), a constant-phase element (Q_{dl}), a polarization resistance (R_t) and a Warburg component (W). The Warburg impedance is usually observed at low frequencies in electrochemical experiments due to the concentration polarization induced by a sluggish diffusion process. The circuit parameters are approximately determined by fitting the experimental data with the equivalent circuit and tabulated in Table 2. In Table 2, factor n_{dl} represents the Q_{dl} power, which is usually between 0.5 and 1[19]. When n_{dl}=1, a Q_{dl} is equivalent to an ideal capacitor. The EIS analysis shows that the polarization resistance (R_t) of the MAE barrel-plated Ni-P coating is higher than that of the CE-plated Ni-P coating, thereby indicating again that the corrosion resistance is improved by the mechanical *in situ* treatment. After heat treatment, the values of R_t are decreased slightly for both CE-plated coating and MAE barrel-plated coating, which is consistent with the negative shift of the corrosion potential.

4. Discussion

From the surface observations and surface roughness measurements, we can see that as the mechanical attrition action is applied to Ni-P barrel-plating, the surface of Ni-P coating becomes smoother. In addition, mechanically assisted electroless barrel-plating would influence the growth of deposits on the coating surface. Therefore, under mechanical attrition action, mechanically assisted electroless barrel-plated Ni-P coating shows a fine microstructure and no pores and cracks compared with the conventional electroless plating process.

Amorphous alloys are of meta-stable phases in a thermodynamic sense and will be crystallized to reach the equilibrium state through annealing. Amorphous Ni-P coating is crystallized to fcc Ni and Ni_3P phases after heat treatment at 400°C for 1 h[20]. The as-deposited Ni-P coating by MAE barrel-plating consists of Ni polycrystals but does not precipitate the phase of Ni_3P, which indicates that the energy produced by mechanical *in situ* treatment could promote the crystallization of the amorphous, but this crystallization might be partial. When Ni and P atoms are deposited on the substrate at room temperature, the meta-stable amorphous state might be at the local energy minimum so that the CE-plated Ni-P coating is amorphous. In addition, the surface diffusion of Ni and P atoms might play a critical role in the formation of the amorphous coating. Under the CE-plating condition, the mobility of deposited Ni and P atoms might be too low, so the Ni and P atoms could not overcome the energy barrier to be crystallized. With the mechanical *in situ* treatment, the balls impact on the deposited coating and thus exert a mechanical

Table 2 Fitting results of EIS of the carbon steel, the CE-plated Ni-P coating and the MAE barrel-plated Ni-P coating

Sample	$R_s/\Omega\cdot cm^2$	$R_{ct}/\Omega\cdot cm^2$	$Q_{dl}/F\cdot cm^{-2}$	n_{dl}	W
Carbon steel	3.389±1%	1066±2%	7.244×10^{-4}±0.3%	0.7852±1.2%	6.317×10^{19}±12%
CE-plated Ni-P coating after heat treatment	3.47±1.3%	1582±2.6%	1.086×10^{-4}±0.2%	0.9757±1.4%	1.256×10^{8}±10%
CE-plated Ni-P coating before heat treatment	3.50±1.6%	1614±3%	1.106×10^{-4}±1%	0.7514±1.7%	1.561×10^{8}±11%
MAE barrel-plated Ni-P coating after heat treatment	0.9136±1%	2025±2.1%	1.742×10^{-4}±0.4%	0.9782±1.5%	2.717×10^{11}±15%
MAE barrel-plated Ni-P coating before heat treatment	1.088±1%	2187±2%	2.127×10^{-5}±1%	0.9876±1%	8.8884×10^{4}±17%

force on the coating. Under such *in situ* mechanical force, the energy barrier for crystallization is greatly reduced. The detailed thermodynamics analysis was reported in a previous literature [21]. The uncompleted crystallization and the lack of Ni_3P phase in as-deposited coating electroless-plated with the mechanical *in situ* assistance might indicate a hypothesis that the mobility of Ni and P atoms might not be enhanced too much by the mechanical *in situ* treatment.

The increase in hardness of the mechanically assisted electroless barrel-plated Ni-P coating might be attributed to the compact and fine grained structure and the extra solid solution hardening of P. Phase transformation and micro-crystallization induced by mechanical attrition might be mainly responsible for the hardness increase.

After heat treatment, cracks are observed in the CE-plated Ni-P coating, indicating that a tension stress field is built up. This fact means the volume shrinkage during the crystallization of the amorphous coating. Since the MAE barrel-plated Ni-P coating has been crystallized, its density must be higher than that of the CE-plated coating. Therefore, the volume change during the heat treatment must be much smaller in the MAE barrel-plated Ni-P coating than that in the CE-plated coating so that no cracking occurs. After heat treatment, as described above, the grain sizes of Ni and Ni_3P in the MAE barrel-plated Ni-P coating are all smaller than those in the CE-plated coating, respectively. Thus, the hardness, the corrosion resistance and the wear resistance would be greatly improved by the mechanical *in situ* treatment.

5. Conclusion

In summary, a novel coating process, *i.e.* the MAE barrel-plating, has been developed to deposit Ni-P coatings on carbon steel. The Ni-P coatings possess smooth surfaces and a fine grained structure. The coating properties including hardness and corrosion resistance have been improved effectively. No cracks in the MAE barrel-plated Ni-P coatings are formed after heat treatment at 400°C for one hour. These excellent properties produced by the mechanical *in situ* treatment will bring wide applications of the MAE barrel-plating technique to engineering practice.

Acknowledgement

This work was financially supported by the National Natural Science Foundation of China (No. 50671006).

REFERENCES

[1] D.W. Baudrand: *Electroless Nickel Plating,* ASM Handbook, Vol. 5, ASM International, Materials Park, OH, 1994, 290.
[2] Y.Z. Zhang and M. Yao: *Trans. Inst. Metal Finish.,* 1999, **77**(2), 78.
[3] R.R. Tummala, E.J. Rymaszeski and A.G. Klopfenstein: *Microelectronics Packaging Handbook,* Part 2, Chapman and Hall, London, 1997, Chapter 8.
[4] S.V.S. Tyagi, S.K. Barthwal, V.K. Tandon and S. Ray: *Thin Solid Films,* 1989, **169**(2), 229.
[5] P.S. Kumar and P.K. Nair: *J. Mater. Process. Technol.,* 1996, **56**, 511.
[6] N.M. Martyak and K. Drake: *J. Alloy. Compd.,* 2000, **312**, 30.
[7] E.M. Ma, S.F. Luo and P.X. Li: *Thin Solid Films,* 1988, **166**, 273.
[8] R.C. Agarwala and S. Ray: *Z. Metallkd.,* 1989, **80**(8), 556.
[9] K.H. Hur, J.H. Jeong and D.N. Lee: *J. Mater. Sci.,* 1991, **26**(8), 2037.
[10] K. Parker: *Plat. Surf. Finish.,* 1981, **68**(12), 71.
[11] A.W. Goldenstein, W. Rostoker and F. Schossberger: *J. Electrochem. Soc.,* 1957, **104**(2), 104.
[12] R. Narayan and M.N. Mungole: *Metal Finish.,* 1985, **83**(11), 55.
[13] M.H. Staia, E.J. Cadtillo, E.S. Puchi, B. Lewis and H.E. Hintermann: *Surf. Coat. Technol.,* 1996, **86-87**, 598.
[14] J.Y. Song and J. Yu: *Thin Solid Films,* 2002, **415**, 167.
[15] R.S. Razavi, M. Salehi, M. Monirvaghefi and G.R. Gordani: *J. Mater. Process. Technol.,* 2009, **69**, 112.
[16] P.H. Tremmel: *Finish. Equipment,* 1985, **34**, 602.
[17] Y. He, H. Fu, X. Li and W. Gao: *Scripta Mater.,* 2008, **58**, 504.
[18] L.S. Birks and H. Friedman: *J. Appl. Phys.,* 1946, **17**, 687.
[19] Z. Guo, K.G. Keong and W. Sha: *J. Alloy. Compd.,* 2003, **358**, 112.
[20] K.G. Keong, W. Sha and S. Malinov: *J. Mater. Sci.,* 2002, **37**, 4445.
[21] Z. Ping, Y. He, C. Gu and T. Zhang: *Surf. Coat. Technol.,* 2008, **202**, 6023.